Received: 24 March 2023 | Revised: 25 May 2023 | Accepted: 10 July 2023

DOI: 10.1002/jor.25661

Journal of Orthopaedic Research®

RESEARCH ARTICLE

Foot kinematics as a function of ground orientation and weightbearing

Michele Conconi[1] | Alessandro Pompili[1] | Nicola Sancisi[1] | Stefano Durante[2] | Alberto Leardini[3] | Claudio Belvedere[3]

[1]Department of Industrial Engineering—DIN, University of Bologna, Bologna, Italy

[2]Area Tecnico Diagnostica Radiologica, IRCCS S. Orsola Malpighi Hospital, Bologna, Italy

[3]Movement Analysis Laboratory, IRCCS Istituto Ortopedico Rizzoli, Bologna, Italy

Correspondence
Michele Conconi, Viale del Risorgimento 2, 40139 Bologna, Italy.
Email: michele.conconi@unibo.it

Funding information
This study was partially funded by the Italian Ministry of Health under the "5 per mille" program."; Italian Ministry of Health under the "5 per mille" program

Abstract

The foot is responsible for the bodyweight transfer to the ground, while adapting to different terrains and activities. Despite this fundamental role, the knowledge about the foot bone intrinsic kinematics is still limited. The aim of the study is to provide a quantitative and systematic description of the kinematics of all bones in the foot, considering the full range of dorsi/plantar flexion and pronation/supination of the foot, both in weightbearing and nonweightbearing conditions. Bone kinematics was accurately reconstructed for three specimens from a series of computed tomography scans taken in weightbearing configuration. The ground inclination was imposed through a set of wedges, varying the foot orientation both in the sagittal and coronal planes; the donor body-weight was applied or removed by a cable-rig. A total of 32 scans for each foot were acquired and segmented. Bone kinematics was expressed in terms of anatomical reference systems optimized for the foot kinematic description. Results agree with previous literature where available. However, our analysis reveals that bones such as calcaneus, navicular, intermediate cuneiform, fourth and fifth metatarsal move more during foot pronation than flexion. Weightbearing significantly increase the range of motion of almost all the bone. Cuneiform and metatarsal move more due to weightbearing than in response to ground inclination, showing their role in the load-acceptance phase. The data here reported represent a step toward a deeper understanding of the foot behavior, that may help in the definition of better treatment and medical devices, as well as new biomechanical model of the foot.

KEYWORDS
anatomical reference systems, foot kinematics, ground orientation, weightbearing

1 | INTRODUCTION

The foot-ankle complex is a multiarticulated system that plays a fundamental role in human locomotion, mediating the interaction between lower limb and the ground. For this reason, its mechanical behavior is of high clinical interest. Due to the number of bones participating to the complex, a thorough description of the foot bone and joint kinematics is, however, challenging.

The early quantifications of foot motion were focused on locating mean helical axes and corresponding rotations at a number

of joints.[1–4] Although clinically relevant, this simplification does not provide a full characterization of the three-dimensional behavior of the joint in the foot, whose motion differs from ideal hinges. Later, detailed quantifications of the three-dimensional kinematics of foot bones were provided, introducing joint coordinates systems to track and report bone displacement with six degrees of freedom, although limited to specific foot joints (i.e., mainly the talar, subtalar and talo-navicular joints).[5–10]

With modern gait analysis, the foot-ankle kinematics was measured with stereophotogrammetric systems and skin markers under different load conditions.[10,11] With this approach it is, however, impossible to follow the motion of all the bones, which were therefore grouped into rigid clusters.[12] Also, the inaccuracies related to skin-motion artifact make this approach unsuitable for the measurement of the fine midtarsal and tarsal motion.

More recently, several researchers investigated the foot through fluoroscopy.[13] Despite the accuracy and the potentiality offered by this technique, its application is often limited to the hindfoot, with some exception including the midtarsal joint,[14,15] or the first[16] and fifth metatarsal bones,[17] mainly due to the challenges in 2D/3D registration provided by the overlapping X-ray projections of the bones in the foot.

Foot kinematics was also investigated through magnetic resonance imaging (MRI), both as a sequence of static poses[18–20] or by means of dynamic MRI.[21,22] The first approach is, however, limited by the segmentation time, while the second is an emerging yet still developing technique, whose application has been limited to the hindfoot so far.[23]

Intracortical pins are an accurate yet invasive tool for the tracking of multiple bones. Arndt and co-workers exploited this approach, investigating the in vivo kinematics of the midtarsal foot together with the first and fifth metatarsals, during gait[24] and slow running.[25] Later, Nester and co-workers[26] presented the first complete in vitro investigation of the whole foot and ankle complex kinematics, using intracortical pins in combination with a walking simulator. The study was then replicated in vivo, with the exclusion of the intermediate and lateral cuneiforms, as well as second, third, and fourth metatarsals, to limit invasiveness.[27] These studies defined bone reference systems as parallel to the global foot frame (at a neutral foot configuration). This simplified the analyses of foot kinematics and range of motion (ROM), however, information about the absolute position and orientation of foot bones (hereinafter referred as "foot posture") is lost. Whittaker and co-workers overcame this limitation by introducing anatomical reference systems (ARS) for each bone while measuring their motion by means of intracortical pins and a gait simulator.[28]

More recently, the advent of weightbearing scanning techniques raised the interest in a better understanding of how load affects foot motion.[29] Ito and co-workers provided a detailed in vitro quantification of the effect of an increasing vertical load on the foot, including all the bones but the cuneiforms.[30] However, only the neutral posture was analysed.

Despite the considerable literature on the topic, the knowledge about foot bones' motion is still partial: a comprehensive description of foot kinematics and ROM considering both dorsi/plantar flexion and pronation/supination of the foot as well as the variation introduced by weightbearing is still lacking. In part this is also due to the absence of standardized reference systems for the foot bones, making the comparison with previous data complex,[31] and often resulting in a suboptimal description of bone kinematics, introducing cross-talk among the various motion components.[32]

The aim of the study is to fill the gap, by providing a quantitative, systematic and comprehensive description of foot bone kinematics. The full range of foot dorsi/plantar flexion and pronation/supination is considered, both in weightbearing and nonweightbearing conditions to show the effect of loads on the foot kinematics and posture. Foot bone kinematics is reconstructed in vitro from a series of computed tomography (CT) scans both with and without a vertical load insisting on the ankle, by resorting to ARS optimized for the foot kinematics description.[33] To frame the results of the present analysis with respect to the previous literature, at the same time enlightening the impact of the chosen ARS, bone kinematics and ROM will be quantified with respect to the neutral foot posture, expressing our findings also in terms of the most commonly choice of reference systems adopted so far in the literature.[24–27]

2 | MATERIALS AND METHODS

2.1 | Data collection

We analysed three fresh-frozen full lower left limbs (male; age: 77.7 ± 7.8 years; height: 175.3 ± 5.8 cm; weight: 87.0 ± 15.7 Kg). Each specimen was thawed for more than 36 h prior the tests. Cone Beam CT scans (OnSight Extremity System, Carestream®; isotropic voxel-0.26 mm, FOV-230 × 230 mm) were acquired and inspected by a surgeon, who confirmed the absence of previous pathologies. Legs were then casted with the knee extended, leaving only the ankle and foot free to move. To compensate for the in vitro tendon rigidity, the Achilles tendon was resected to increase the range of dorsi/plantar flexion to physiological values. The so prepared specimen was then analysed through the same CBCT scanner. The ankle dorsi/plantar flexion was varied among five values (−30°, −10°, 0°, 10°, and 20°) and foot pronation/supination among three values (−10°, 0°, and 10°), for a total of 15 different foot orientations, using a series of wooden wedges (Figure 1A–F). This foot ROM was chosen to be representative of physiological ROM[34] and repeatable on all specimens. The leg axis was kept vertical by means of a supporting jig (Figure 1G), without introducing additional constraints. These 15 foot orientations were scanned first in the absence of load (nonweightbearing): a cable system connected the casted leg to the supporting jig, and cable lengths were adjusted to guarantee the foot-ground contact with minimal load. The same 15 scans were then repeated in weightbearing, i.e. by adding a vertical axial load equal to half the donor's bodyweight, insisting on the femoral neck (Figure 1G). Two additional scans were performed by rotating the leg internally and externally through the same cable system, starting

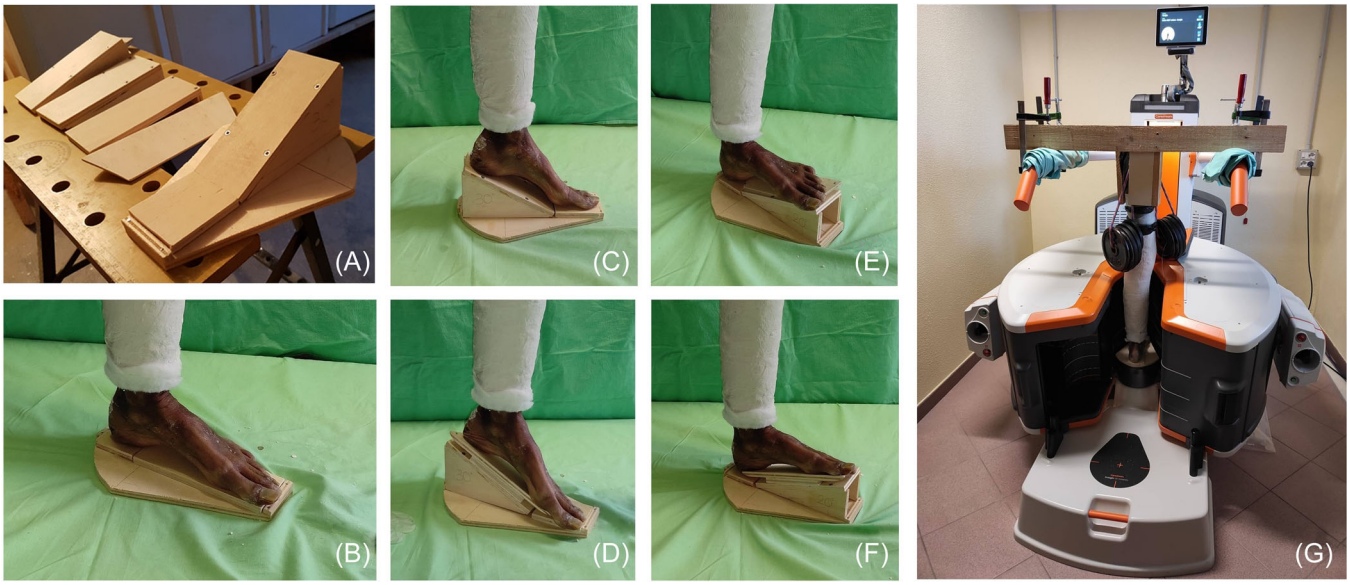

FIGURE 1 Experimental setup and cadaveric foot conditions: (A) wooden wedges to impose foot postures (B–F); (G) wooden jig for leg support and application of vertical axial load, within the gantry of the cone-beam CT scanner. CT, computed tomography.

from the foot neutral posture: the leg was rotated to the limit value that preserves the contact of the whole foot sole with the ground. A total of 32 scans were thus acquired for each leg.

2.2 | 3D bone models reconstruction

For each scan, 3D bone models of the fourteen bones of the foot were reconstructed. Segmentation was carried out through a semi-automatic procedure developed in MITK software (Medical Imaging Interaction Toolkit, German Cancer Research Center - DKFZ): firstly, bones were identified by a single, lower bound threshold, whose value was chosen between 280 and 400 Hounsfield Units to minimize the overlap among bones (Figure 2A). If necessary, voxels were manually removed to separate the bones or added to guarantee continuity in the cortical surface (Figure 2B). Then, each bone segmentation was completed by two morphological operations: closing (structuring element: ball; radius:18 mm) and filling (Figure 2C). Finally, STL file with 3D bone models were created from the segmentations (Figure 2D). This semi-automatic procedure required about 2 h per scan to a trained operator. To validate the accuracy of this process, TA, CI, M1 were also segmented manually from one scan for each leg, and the DICE score between semiautomatic and manual segmentation was calculated.

2.3 | Quantification of average articular kinematics and ROM

To describe bone kinematics, we first defined ARS using the functional approach recently proposed by these authors[33] (Figure 3A,B). To compare the results with the literature,[24–27] we also defined additional reference systems for each bone, parallel to the tibia ARS at the foot neutral posture (0° dorsi/plantar flexion, 0° pronation/supination, unloaded) and with the origin coincident with the bone centroid (Figure 3C,D), hereinafter denoted as Tibia-Parallel Reference System (TPRS). In both cases, x, y, z axes are approximatively oriented anteriorly, proximally and to the right. Bone 3D orientation was expressed through a variation of the classic Grood & Suntay cardanic sequence,[35] optimized for the foot: for the relative motion between two bones, dorsi/plantar flexion is the rotation about the z-axis of the proximal bone, pronation/supination is the rotation about the x-axis of the distal bone, abduction/adduction is the rotation about the axis perpendicular to the previous two. Bone position was represented by means of the coordinates of the reference system origin.

Through an automatic, ICP based registration algorithm, foot kinematics was obtained by registering each bone 3D model including the ARS and TPRS to the corresponding bone model automatically segmented at each scan. This resulted in 32 roto-translational matrixes for each bone, then converted into rotational and translational coordinates.

To assess the accuracy of the overall procedure for kinematics reconstruction, bone motion was simulated for three bones (TA, IC, and M1) of the three subjects. A set of five synthetic scans were obtained by applying five rigid rototranslations to the DICOM voxels of the neutral posture scan. The transformations were chosen randomly within the foot ROM. These virtual scans were reinterpolated and then segmented as previously described, finally registering the STL bone models from anatomical to the virtual poses. This bone motion was then compared with the imposed one, measuring orientation and translational error as the norm of angular and positional coordinates error.

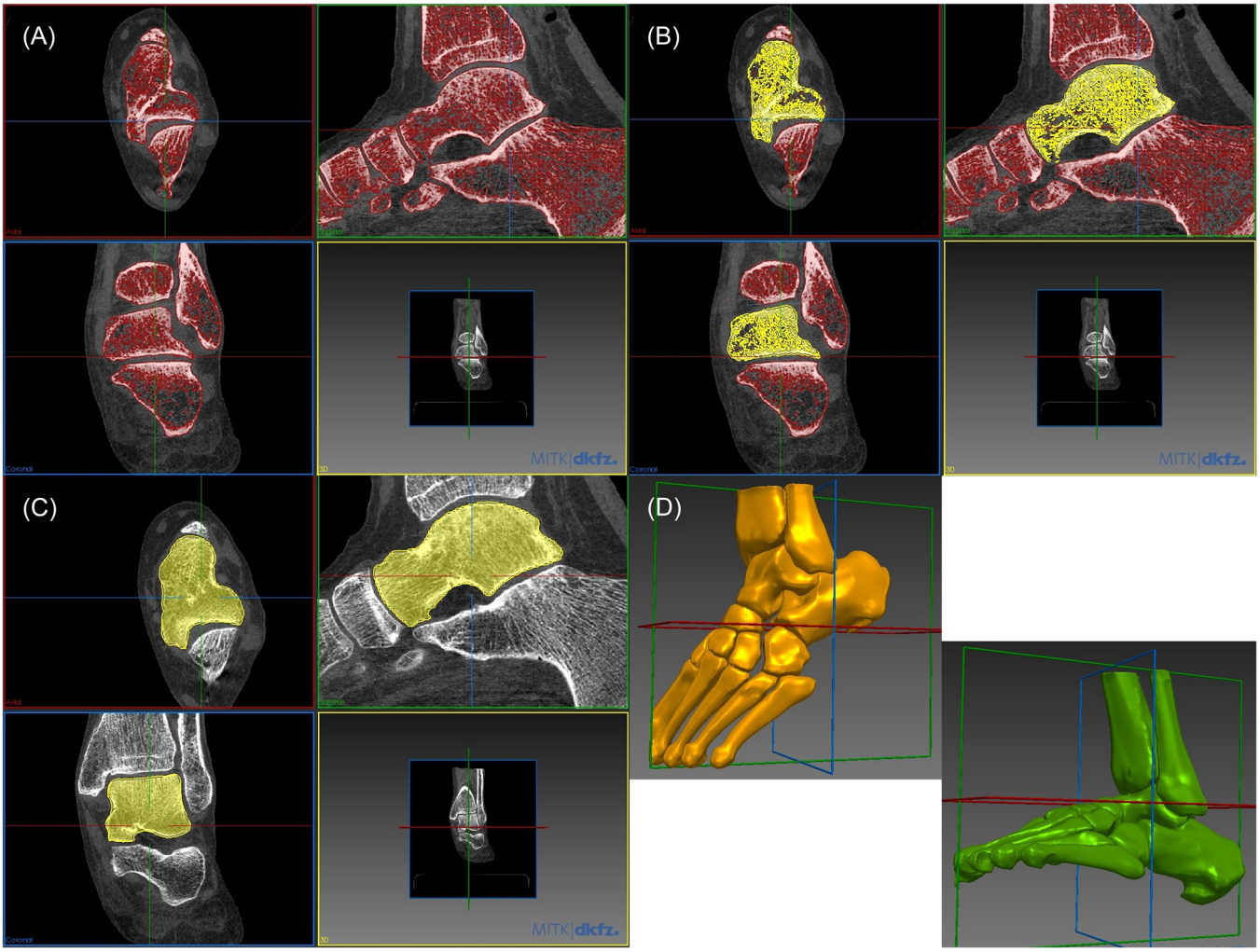

FIGURE 2 3D bone model reconstruction: (A) bone identification through thresholding; (B) manual identification of the talus; (C) morphological operations (closing and filling) to complete bone segmentation; (D) final 3D bone models in STL files.

The relative kinematics between all the articulating pairs of bones was computed for each subject using the rototranslational matrixes coming from the ICP registration. For the sake of simplicity and for comparison with the previous literature, bone kinematics was normalized with respect to the neutral foot posture, i.e. by computing the variation of each bone motion component with respect to this posture. The ROM was defined for each motion component as the difference between the maximum positive and negative values. Data were obtained for both the ARS and TPRS, to point out the effect of the reference system on the description of foot kinematics and to compare the results of the present analysis with the literature. Only orientation was considered in this paper, but all data are reported in the additional material, also showing the relative kinematics before the normalization for the sake of completeness.

To identify how the load affected foot motion, repeated measures analysis of variance was used to compare nonweightbearing and weightbearing bone kinematics, considering each motion component and joint independently. To cope with the small number of subjects, significance was set to $p \leq 0.01$, thus below the standard 0.05.

3 | RESULTS

As for the quality of the semiautomatic registration, the minimum and maximum DICE scores were observed for the CI (95.9%) and the TA (98%). The average DICE score was 96.9% ± 07, higher than what typically found in the literature for fully automated segmentation algorithms.[36]

The accuracy of the kinematic reconstruction procedure was evaluated as the overall rotational and translational mean absolute error (MAE) for the simulated foot motion: rotational MAE was 0.34 ° ± 0.39°, while translational MAE was 0.10 ± 0.13 mm. The highest registration errors were observed for the CI bone (0.53° ± 0.23° and 0.14 ± 0.09 mm), while the lowest values were found for TA (0.16° ± 0.10° and 0.09 ± 0.09 mm). These values are comparable with those obtainable using video-fluoroscopy technique for the quantification of the foot bone motion (see for instance Ito et al.[14]).

The average ROM in nonweightbearing (NW) and weightbearing (W) conditions for all the joints are divided according to the foot section: rearfoot (Table 1), midfoot (Table 2), and forefoot (Table 3).

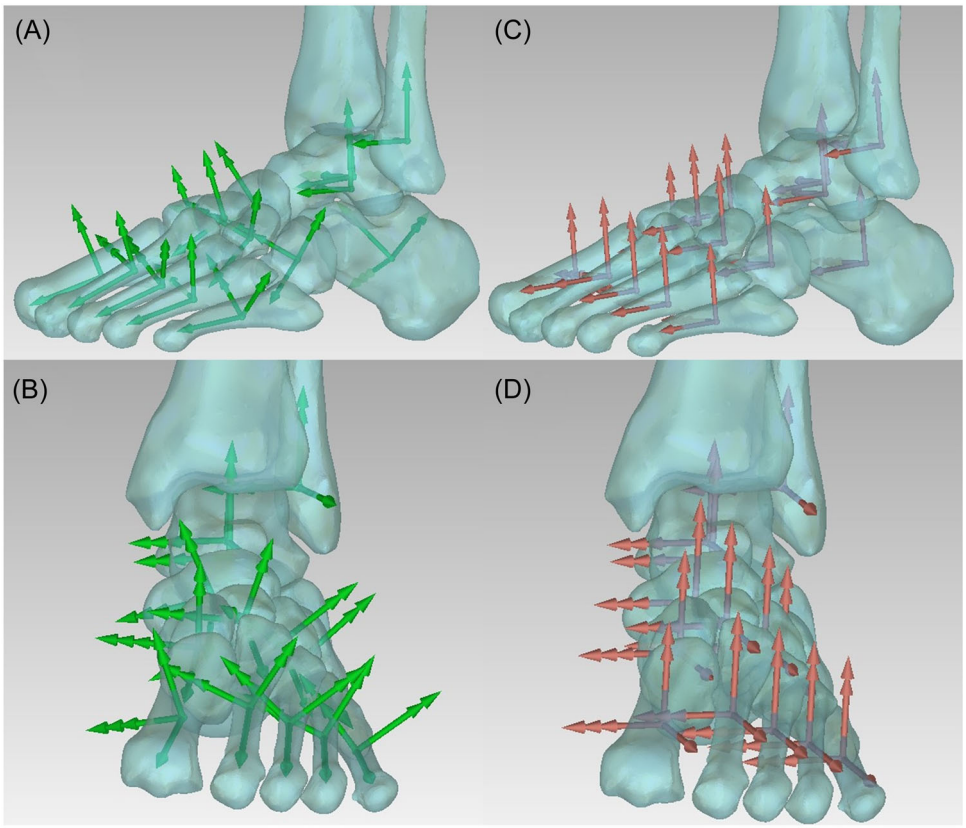

FIGURE 3 Representation of the different bone reference systems: ARS defined according to,[33] (A, B); TPRS used in the previous literature,[24–27] (C, D). Single pointed arrows denote x axes; double pointed arrows denote y axes; triple pointed arrows denote z axes. TPRS, Tibia-Parallel Reference System.

TABLE 1 Average ROM, with upper and lower bound (UB, LB) with respect to the neutral foot posture, for joints in the **rearfoot** in nonweightbearing (NW) and weightbearing (W) conditions.

	FI-TI		TA-TI		CA-TA	
	NW	W	NW	W	NW	W
Dorsi/plantar flexion [°]						
ROM	0.8 ± 0.1	1.3 ± 0.5	47.6 ± 3.0	**50.1 ± 2.8**	2.1 ± 0.9	**3.2 ± 1.3**
UB	0.3 ± 0.3	0.5 ± 0.0	19.2 ± 2.1	19.9 ± 3.2	0.8 ± 0.9	1.5 ± 1.3
LB	−0.5 ± 0.3	−0.8 ± 0.5	−28.4 ± 4.7	−30.2 ± 4.0	−1.3 ± 0.7	−1.6 ± 1.3
Pronation/supination [°]						
ROM	0.8 ± 0.3	1.3 ± 0.5	2.5 ± 1.0	4.9 ± 2.1	12.3 ± 5.5	**24.9 ± 6.3**
UB	0.2 ± 0.2	0.5 ± 0.2	1.1 ± 0.1	1.3 ± 0.3	3.6 ± 3.5	7.0 ± 3.2
LB	−0.6 ± 0.1	−0.8 ± 0.3	−1.4 ± 1.1	−3.6 ± 2.3	−8.7 ± 4.4	−17.9 ± 5.6
Abduction/adduction [°]						
ROM	2.7 ± 1.2	**3.3 ± 1.4**	9.3 ± 3.4	10.8 ± 2.4	2.6 ± 1.6	3.9 ± 1.8
UB	1.3 ± 1.3	1.8 ± 0.7	5.7 ± 1.7	5.9 ± 2.1	1.5 ± 1.5	2.1 ± 1.5
LB	−1.4 ± 1.1	1.5 ± 1.1	−3.6 ± 2.7	−4.9 ± 1.4	−1.1 ± 0.6	−1.8 ± 0.7

Note: Bold numbers denote components for which weightbearing induced significant differences on the bone mobility.
Abbreviation: ROM, range of motion.

TABLE 2 Average ROM, with upper and lower bound (UB, LB) with respect the neutral foot posture, for joints in the **midfoot** in nonweightbearing (NW) and weightbearing (W) conditions.

	NA-TA		CU-CA		CU-NA		CM-NA		CI-NA		CL-NA		CI-CM		CL-CI		CU-CL	
	NW	W	NW	W	NW	W	NW	W	NW	W	NW	W	NW	W	NW	W	NW	W
Dorsi/plantar flexion [°]																		
ROM	5.3 ± 3.2	**7.7 ± 4.6**	2.4 ± 1.4	3.3 ± 1.3	2.7 ± 0.9	3.9 ± 1.6	8.5 ± 1.3	**12.2 ± 4.7**	4.7 ± 0.8	**6.2 ± 2.4**	3.3 ± 0.2	**4.3 ± 0.9**	3.5 ± 1.1	**5.1 ± 1.6**	2.8 ± 1.4	**3.7 ± 1.3**	3.7 ± 1.8	5.0 ± 2.2
UB	1.4 ± 1.5	3.8 ± 3.0	0.9 ± 0.6	1.2 ± 0.7	0.7 ± 0.5	1.3 ± 1.2	2.7 ± 1.8	5.1 ± 3.0	1.5 ± 1.3	2.7 ± 2.2	1.2 ± 0.4	2.2 ± 0.9	2.5 ± 1.1	3.1 ± 1.0	1.4 ± 0.8	1.4 ± 0.8	2.4 ± 1.2	3.3 ± 2.0
LB	−3.9 ± 1.8	−3.9 ± 1.8	−1.5 ± 1.1	−2.0 ± 0.7	−1.9 ± 0.6	−2.6 ± 0.4	−5.8 ± 2.2	−7.1 ± 2.6	−3.2 ± 0.6	−3.5 ± 0.5	−2.1 ± 0.5	−2.2 ± 0.6	−1.0 ± 0.4	−2.0 ± 0.7	−1.4 ± 1.0	−2.4 ± 0.7	−1.4 ± 0.8	−1.7 ± 0.5
Pronation/supination [°]																		
ROM	13.8 ± 4.1	**20.4 ± 9.3**	5.3 ± 2.7	6.7 ± 4.0	6.6 ± 1.9	7.7 ± 1.9	4.3 ± 0.5	**6.8 ± 2.0**	4.1 ± 0.9	**6.6 ± 1.1**	2.5 ± 0.6	**6.1 ± 1.2**	2.0 ± 0.8	2.8 ± 0.7	4.1 ± 0.2	**4.6 ± 0.6**	7.5 ± 0.4	8.1 ± 0.4
UB	5.1 ± 2.2	8.1 ± 2.8	3.5 ± 2.9	3.6 ± 2.7	4.2 ± 3.3	4.6 ± 3.9	3.1 ± 0.7	3.6 ± 1.0	3.1 ± 0.6	4.0 ± 1.1	2.2 ± 0.9	3.3 ± 1.7	1.1 ± 0.9	1.3 ± 1.1	2.0 ± 0.8	2.4 ± 1.3	3.9 ± 2.8	4.5 ± 2.6
LB	−8.7 ± 4.8	−12.4 ± 9.3	−1.8 ± 0.2	−3.0 ± 1.3	−2.4 ± 1.6	−3.1 ± 2.0	−1.2 ± 1.0	−3.2 ± 1.6	−1.0 ± 0.6	−2.6 ± 0.5	−0.3 ± 0.4	−2.7 ± 0.7	−0.9 ± 0.1	−1.6 ± 1.1	−2.1 ± 0.7	−2.2 ± 0.7	−3.6 ± 2.6	−3.6 ± 2.6
Abduction/adduction [°]																		
ROM	15.8 ± 6.3	**36.9 ± 9.8**	5.7 ± 1.6	**13.0 ± 2.9**	2.4 ± 0.1	**6.0 ± 3.8**	2.0 ± 0.2	**4.2 ± 1.4**	2.0 ± 0.3	**3.2 ± 1.1**	2.7 ± 0.9	4.0 ± 1.2	3.3 ± 2.5	**3.9 ± 2.0**	2.8 ± 1.3	4.2 ± 0.8	2.9 ± 0.5	**3.7 ± 0.9**
UB	4.8 ± 5.7	10.8 ± 6.8	2.7 ± 1.0	6.6 ± 2.9	1.7 ± 0.5	4.1 ± 3.3	0.7 ± 0.1	2.2 ± 2.2	0.8 ± 0.4	1.9 ± 1.3	1.0 ± 0.3	1.9 ± 0.6	1.4 ± 1.0	1.8 ± 0.5	1.0 ± 1.0	1.7 ± 1.0	1.9 ± 0.8	2.7 ± 1.6
LB	−11.0 ± 3.6	−26.1 ± 9.3	−3.0 ± 0.7	−6.4 ± 3.1	−0.7 ± 0.6	−2.0 ± 0.8	−1.3 ± 0.2	−2.0 ± 1.2	−1.1 ± 0,4	−1.3 ± 0.8	−1.7 ± 1.0	−2.1 ± 0.7	−1.9 ± 1.7	−2.0 ± 1.5	−1.8 ± 0.6	−2.5 ± 1.0	−1.0 ± 1.3	−1.0 ± 1.2

Note: Bold numbers denote components for which weightbearing induced significant differences on the bone mobility.

Abbreviation: ROM, range of motion.

TABLE 3 average ROM, with upper and lower bound (UB, LB) with respect the neutral foot posture, for joints in the **forefoot** in non-weightbearing (NW) and weightbearing (W) conditions.

	M1-CM		M2-CI		M3-CL		M4-CU		M5-CU	
	NW	W	NW	W	NW	W	NW	W	NW	W
Dorsi/plantar flexion [°]										
ROM	2.1 ± 0.9	**3.8 ± 1.7**	2.2 ± 1.6	**4.1 ± 1.1**	2.1 ± 1.4	**4.4 ± 2.9**	8.0 ± 1.9	**12.4 ± 5.7**	12.2 ± 1.6	**15.1 ± 1.6**
UB	0.8 ± 0.2	2.3 ± 0.7	0.0 ± 0.2	2.1 ± 1.5	1.1 ± 0.9	2.2 ± 1.2	4.6 ± 3.9	6.2 ± 3.8	7.5 ± 4.1	8.5 ± 3.0
LB	−1.3 ± 1.1	−1.5 ± 1.0	−2.1 ± 1,4	−2.0 ± 0.8	−1.1 ± 0.6	−2.2 ± 2.5	−3.4 ± 2.3	−6.3 ± 2.1	−4.8 ± 3.5	−6.5 ± 1.9
Pronation/supination [°]										
ROM	3.5 ± 1.9	6.3 ± 2.8	2.4 ± 0.5	3.8 ± 0.5	3.3 ± 0.3	**5.5 ± 1.4**	9.1 ± 3.5	**11.8 ± 4.9**	10.2 ± 2.1	**13.1 ± 4.4**
UB	2.9 ± 2.1	4.1 ± 3.3	2.1 ± 0.6	2.2 ± 0.1	2.4 ± 0.9	3.2 ± 0.7	5.0 ± 2.3	5.0 ± 2.3	4.1 ± 2.7	4.1 ± 2.7
LB	−0.6 ± 0.5	−2.2 ± 1.4	−0.2 ± 0.5	−1.7 ± 0.4	−0.9 ± 0.7	−2.4 ± 1.6	−4.1 ± 5.3	−6.7 ± 6.6	−6.1 ± 3.9	−9.0 ± 6.6
Abduction/adduction [°]										
ROM	3.2 ± 1.8	**6.6 ± 2.7**	4.3 ± 2.5	**6.5 ± 3.1**	3.6 ± 2.0	**5.7 ± 3.9**	6.0 ± 1.0	**7.8 ± 2.5**	3.7 ± 1.8	5.6 ± 2.5
UB	2.1 ± 0.9	3.2 ± 1.3	3.6 ± 2.3	3.1 ± 0.7	2.4 ± 1.5	2.7 ± 2.0	2.9 ± 2.2	2.9 ± 2.2	1.0 ± 1.4	1.9 ± 2.4
LB	−1.1 ± 1.5	−3.5 ± 2.7	−0.7 ± 0.2	−3.4 ± 2.5	−1.2 ± 1.1	−2.9 ± 2.8	−3.2 ± 2.1	−4.9 ± 3.4	−2.7 ± 1.4	−3.8 ± 2.5
	M2-CM		M2-M1		M3-M2		M4-M3		M5-M4	
	NW	W	NW	W	NW	W	NW	W	NW	W
Dorsi/plantar flexion [°]										
ROM	2.3 ± 1.0	3.5 ± 1.1	4.1 ± 2.0	**5.7 ± 2.2**	3.0 ± 0.6	4.4 ± 0.2	6.3 ± 0.2	6.7 ± 0.4	4.2 ± 1.0	**4.7 ± 1.0**
UB	1.4 ± 1.6	2.2 ± 1.9	2.8 ± 2.8	3.1 ± 2.7	1.3 ± 0.2	2.0 ± 0.5	3.3 ± 0.7	3.3 ± 0.7	2.7 ± 0.9	2.8 ± 0.8
LB	−0.8 ± 0.6	−1.3 ± 0.9	−1.3 ± 0.9	−2.6 ± 0.7	−1.7 ± 0.4	−2.5 ± 0.7	−3.0 ± 0.6	−3.5 ± 1.1	−1.5 ± 0.6	−1.9 ± 0.6
Pronation/supination [°]										
ROM	2.1 ± 1.0	3.2 ± 0.5	3.6 ± 2.1	**7.1 ± 2.5**	2.2 ± 0.8	2.6 ± 0.4	4.3 ± 1.5	**5.4 ± 0.8**	3.5 ± 0.7	**4.3 ± 0.7**
UB	1.7 ± 1.2	2.5 ± 1.1	1.7 ± 1.3	4.1 ± 1.2	1.3 ± 1.2	1.3 ± 1.2	2.2 ± 1.1	2.5 ± 0.9	0.9 ± 1.1	1.0 ± 1.3
LB	−0.3 ± 0.3	−0.8 ± 0.6	−1.8 ± 1.3	−3.1 ± 2.5	−0.9 ± 0.8	−1.3 ± 0.9	−2.2 ± 0.7	−2.9 ± 0.4	−2.6 ± 0.5	−3.3 ± 0.6
Abduction/adduction [°]										
ROM	1.9 ± 1.1	4.8 ± 3.3	1.3 ± 0.7	**3.2 ± 2.0**	0.8 ± 0.3	**1.3 ± 0.7**	1.6 ± 0.4	**2.5 ± 0.8**	2.0 ± 0.8	**2.4 ± 0.3**
UB	0.8 ± 0.4	1.9 ± 0.5	0.4 ± 0.4	1.6 ± 1.2	0.4 ± 0.2	0.7 ± 0.6	0.4 ± 0.3	1.0 ± 0.7	1.1 ± 1.0	1.5 ± 0.8
LB	−1.1 ± 1.1	−2.9 ± 2.8	−0.9 ± 0.6	−1.6 ± 1.0	−0.4 ± 0.4	−0.6 ± 0.3	−1.2 ± 0.7	−1.5 ± 0.4	−0.9 ± 0.5	−0.9 ± 0.5

Note: Bold numbers denote components for which weightbearing induced significant differences on the bone mobility.
Abbreviation: ROM, range of motion.

ROM is computed as variation from the foot neutral posture (reported in the additional material, Table S1), using ARS. Motion components for which the vertical load induced statistically significant differences are denoted in bold. In general, weightbearing significantly increases the ROM of almost all the bone and motion components. The same analysis in terms of TPRS is reported in the additional material (Tables S2–S4).

The average nonweightbearing kinematics is depicted in Figures 4, 5, and 6 for the main joint of the hind-, mid- and forefoot, respectively. The variations in the orientation of the moving bone are plotted versus the dorsi/plantar flexion of the foot. Different curves correspond to different values of foot pronation/supination. The average nonweightbearing kinematics of the remaining joints is reported in the additional material (Figures S1 and S2). The analysis reveals that bones such as calcaneus, navicular, intermediate cuneiform, fourth and fifth metatarsal move more as an effect of the pronation than flexion of the foot, showing how some joint in the foot are more involved in adapting the foot posture to different ground orientations. The same plots are also reported according to the TPRS convention (Figures S3–S7).

The motion components on which the load had a significant impact were plotted versus dorsi/plantar flexion of the foot, for different values of foot pronation/supination and both in weightbearing and non-weightbearing conditions. In particular, the most significant load-induced effects at the hindfoot (Figure 7), Chopard joint (Figure 8), cuneiforms (Figure 9), and metatarsal bones

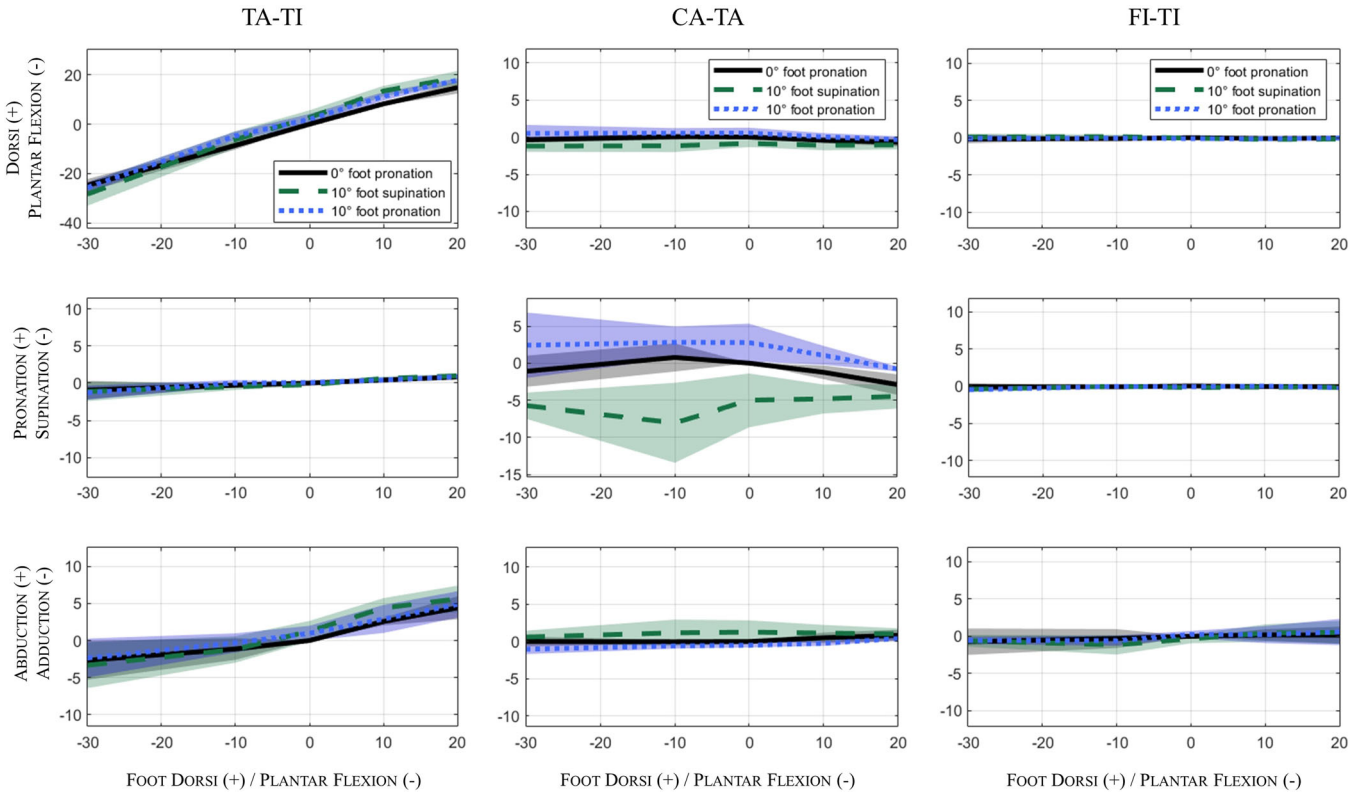

FIGURE 4 Rotational average mobility in nonweightbearing condition, as a function of the dorsi/plantar flexion and pronation/supination of the foot for the three hindfoot joints.

(Figures 10–12) are reported. Interestingly, cuneiform and metatarsal bones move more due to the application of the weight than in response to ground inclination, showing their crucial role in the load-acceptance phase.

The remaining significant effects of weightbearing on bone kinematics are reported in the additional material (Figures S8–S13). For the sake of completeness, the average relative bone kinematics, both in terms of position and orientation, is also reported in the additional material, without normalization with respect to the foot neutral posture (Figures S14.1–S22).

4 | DISCUSSION

In this work, the kinematics and the ROM of all bones in the foot and ankle complex are quantified over the whole range of dorsi/plantar flexion and pronation/supination of the foot, also investigating the variations induced by a vertical load simulating weightbearing.

The talus kinematics with respect to the tibia (TA-TI) shows the previously reported coupling between adduction and plantar flexion, with no significant variation associated with the foot pronation/supination (Figure 4), The load significantly increases the talar flexion, in agreement with what reported in Yamaguchi et al.[37] and with the opening of the medial longitudinal arch under load (Figure 7). However, differently from Yamaguchi et al.,[37] we did not observe statistically significant differences in the TA-TI abduction: this may depend on the higher loading considered in the study of Yamaguchi[37] and co-worker, in which subjects were performing single leg calf rising on a step.

The fibula shows little displacement with respect to the tibia (FI-TI, Table 1), in agreement with the previous literature, although in our case the opening of the tibiofibular mortise was less pronounced that what found in other studies.[38] Load as a significant effect only on the abduction, in particular when the foot is plantar flexed (Figure 7).

The motion of the calcaneus relative to the talus was little affected by the foot flexion, following instead its pronation/supination (Figure 4). The CA-TA kinematics is strongly affected by weightbearing,[10,37] whose application systematically increase the calcaneus pronation (Figure 7) and, to a smaller extent, its flexion relatively to the TA (Figure S8).

The talo-navicular joint (NA-TA) resulted as the most movable in the foot (Table 1), second only to TA-TI in term of ROM.[26–28] Differently from any other joints, NA-TA displaces considerably as a consequence of both foot dorsi/plantar flexion and pronation/supination, being more sensitive to the latter (Figure 5). NA-TA kinematics involves mainly pronation and abduction (Figure 5) and it is significantly affected by weightbearing, which induces a systematic increase in the abduction, pronation and dorsiflexion angles (Figure 8), associated with an opening of the medial longitudinal arch.

The cuboid displaces with respect to the calcaneus (CU-CA) mainly as an effect of foot pronation/supination, moving mainly in abduction/adduction (Figure 5). In weightbearing, CU-CA abduction

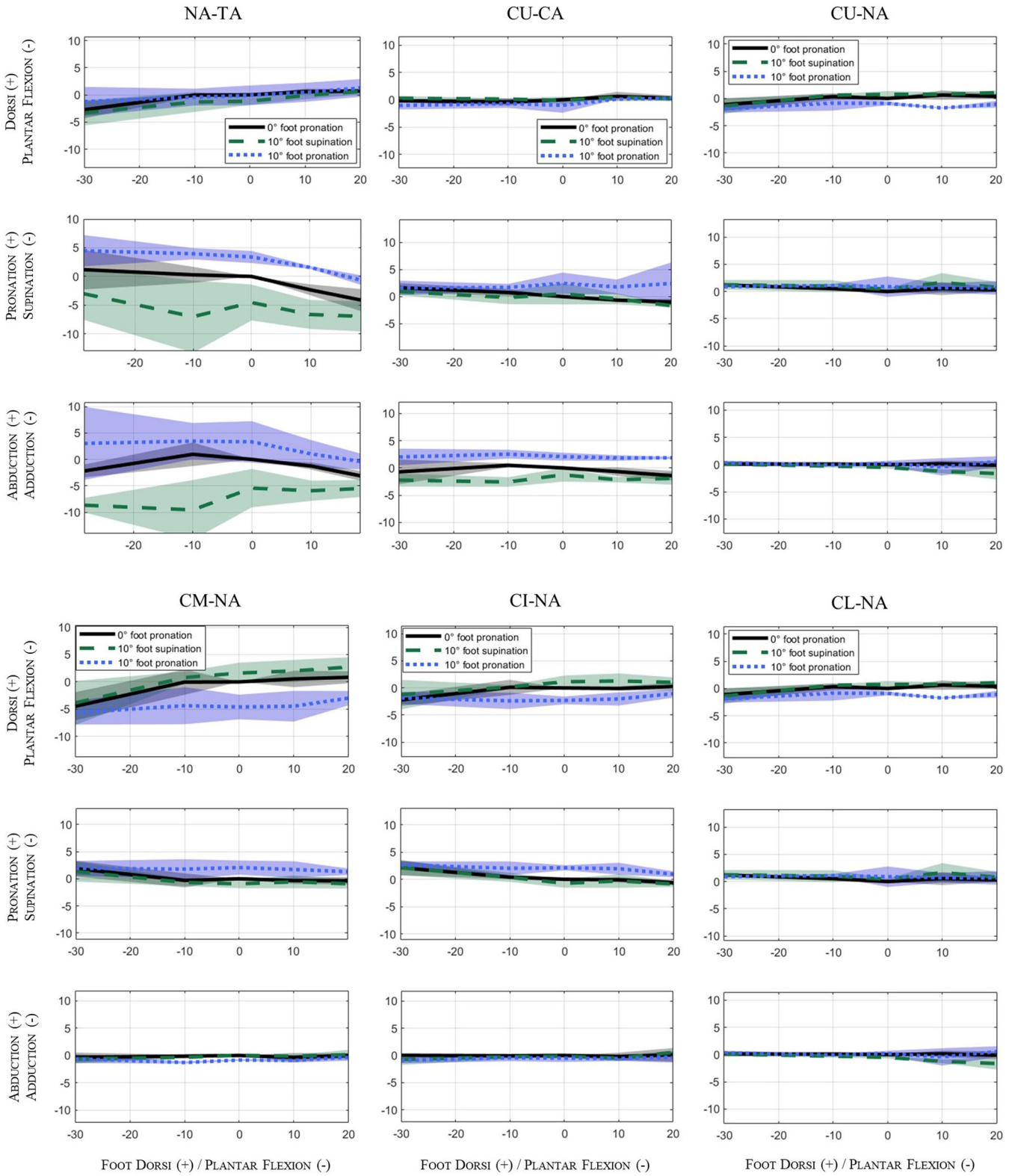

FIGURE 5 Rotational average mobility in nonweightbearing condition, as a function of the dorsi/plantar flexion and pronation/supination of the foot for the main midfoot joints.

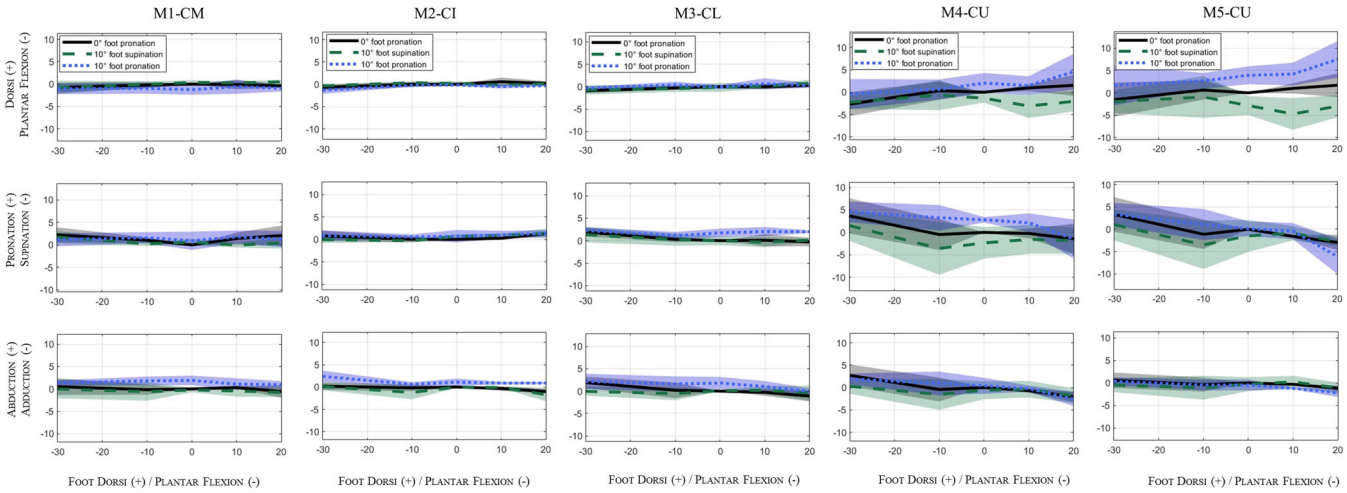

FIGURE 6 Rotational average mobility in nonweightbearing condition, as a function of the dorsi/plantar flexion and pronation/supination of the foot for the main forefoot joints.

increase significantly (Figure 8), resulting in a flattening of the lateral longitudinal arch. Similarly, CU-NA motion resulted quite constrained, being almost insensitive to foot flexion/extension (Figure 5), however, following the pronation/supination motion of the foot.

The cuneiforms mobility with respect to the navicular (CM-NA, CI-NA, CL-NA) decrees progressively from the medial to the lateral one (Table 2), involving mainly dorsi/plantar flexion in association with foot pronation/supination (Figure 5). The lateral cuneiform stays essentially still with respect to the navicular bone. The intercuneiform mobility is in general small, while some degree of pronation/supination is observable between lateral cuneiform and cuboid (CU-CL, Figure S1). However, when load is applied cuneiform mobility increase (Table 2), with a significant effect on almost all the motion components; in particular, weightbearing increase the supination of all the cuneiform with respect to navicular bone, with an effect decreasing from the more movable medial cuneiform to the less movable lateral cuneiform, with CM-NA and CI-NA also showing an increase in dorsiflexion (Figure 9). Overall, the cuneiforms show an interesting response to weight, suggesting an opening of the transversal arch in weightbearing.

First, second, and third metatarsal bone shows reduced mobility with respect to the proximal cuneiforms they articulate with (M1-CM, M2-CI, M3-CL, Table 3). On the contrary, both fourth and fifth metatarsals move significantly with respect to the cuboid, mainly in dorsi/plantar flexion and pronation/supination and in association with the same motion of the foot (M4-CU, M5-CU, Figure 6). Some relative dorsi/plantar flexion is observable between first and second metatarsal, while the relative motion between second and third metatarsal is very small (M2-M1, M3-M2, Figure S2). On the contrary, foot pronation/supination induces a considerable relative dorsi/plantar flexion between fourth and third as well as between fourth and fifth metatarsals (M4-M3, M5-M4, Figure S2). In weightbearing, a significant effect on almost all the metatarsal motion components can be observed. Load increases the dorsiflexion of all the metatarsal bones with respect to cuneiforms, with a higher effect on M4-CU and M5-CU (Figure 10). Similarly, weightbearing is associated with adduction for all metatarsal but M5 (M1-CM, M2-CI, M3-CL, M4-CU, Figure 11). Load is also associated with an increase in supination whose effect rises from M3-CL to M5-CU (Figure 12). Globally, the weightbearing results in a flattening of the forefoot, with a significant displacement involving M4 and M5.

It is interesting to observe that, dorsi/plantar flexion is localized mainly at the TA-TI joint, involving to some minor extent the NA-TA, CI-NA, M4-CU and M5-CU joint (Figures 4–6). The remaining joints shows indeed kinematics curves that do not vary with the orientation of the foot in the sagittal plane Thus, the mobility of many bones is little affected by the foot dorsi/plantar flexion. On the other side, several joints are more responsive to the pronation/supination of the foot, such as CA-TA, CU-CA, CL-NA, CL-CI, CU-CL, M4-M3, M5-M4 (Figures 4, 5, S1, S2). Overall, this analysis reveals the fundamental role of the intrinsic foot motion in adapting to the ground orientation in the coronal plane, a topic that deserve further investigations.

The comparison between weightbearing and non-weightbearing kinematics allows a deeper analysis of load effects on foot behavior. Weightbearing resulted in a general increase of the ROM, in most cases introducing an offset with respect to the non-weightbearing curves, however, without altering the overall motion pattern. This can be account for the elastic deformation of the foot arches under load. Also, this comparison makes it possible to identify the bones more involved in weightbearing. Indeed, cuneiform and metatarsal bones move more due to weightbearing than in response to ground inclination (Figures 9 and 10), showing their key role in the load-acceptance phase. Again, further analysis is needed to deepen the comprehension of the load effect on foot bone kinematics, supporting the crucial role of the emerging weightbearing CT technologies.[39]

Our quantification of ROM is in substantial agreement with the previous literature, when expressed in terms of TPRS for the sake of

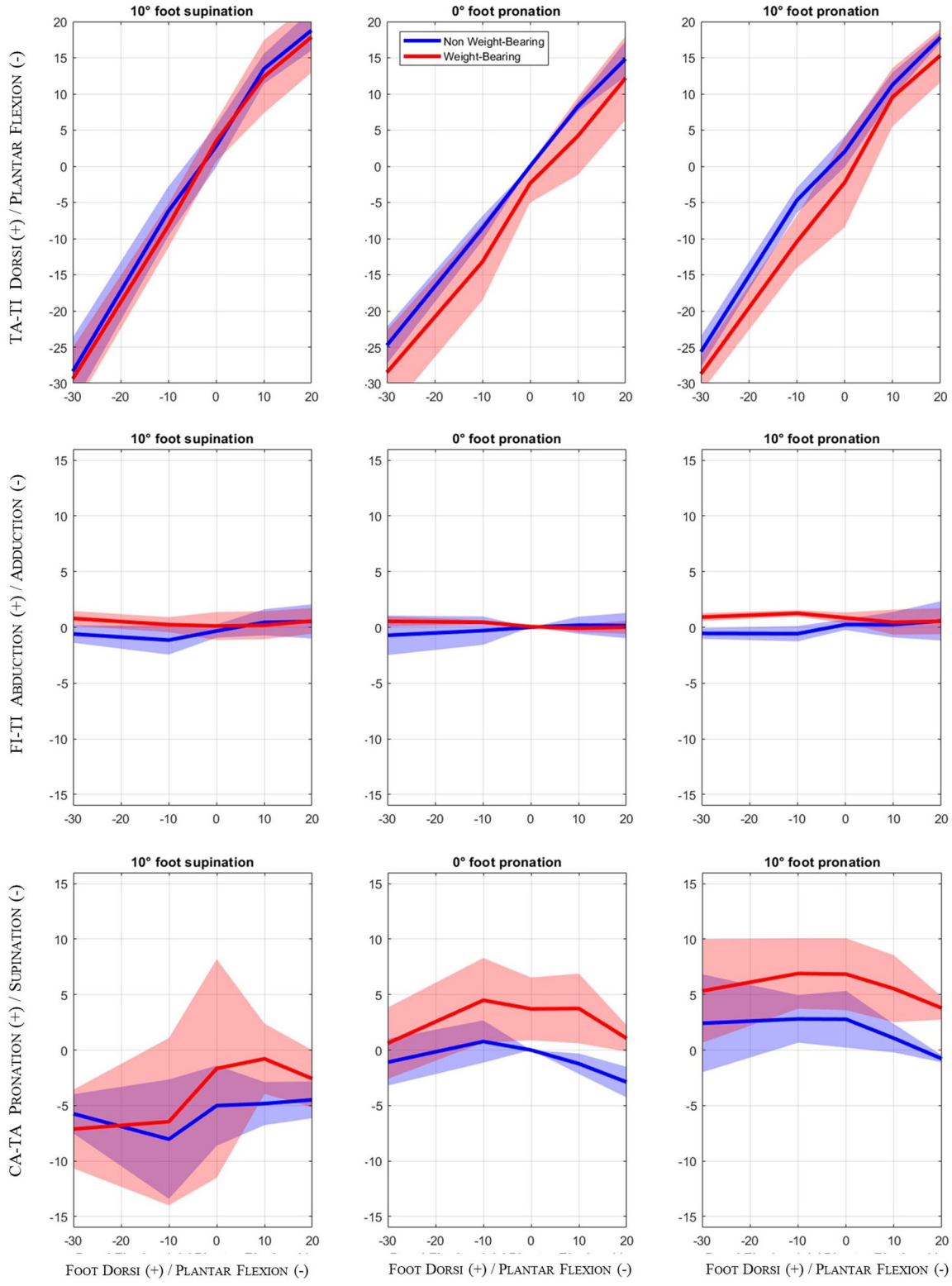

FIGURE 7 Statistically significant differences between nonweightbearing and weightbearing average rotational mobility for the main motion components at the hindfoot joints.

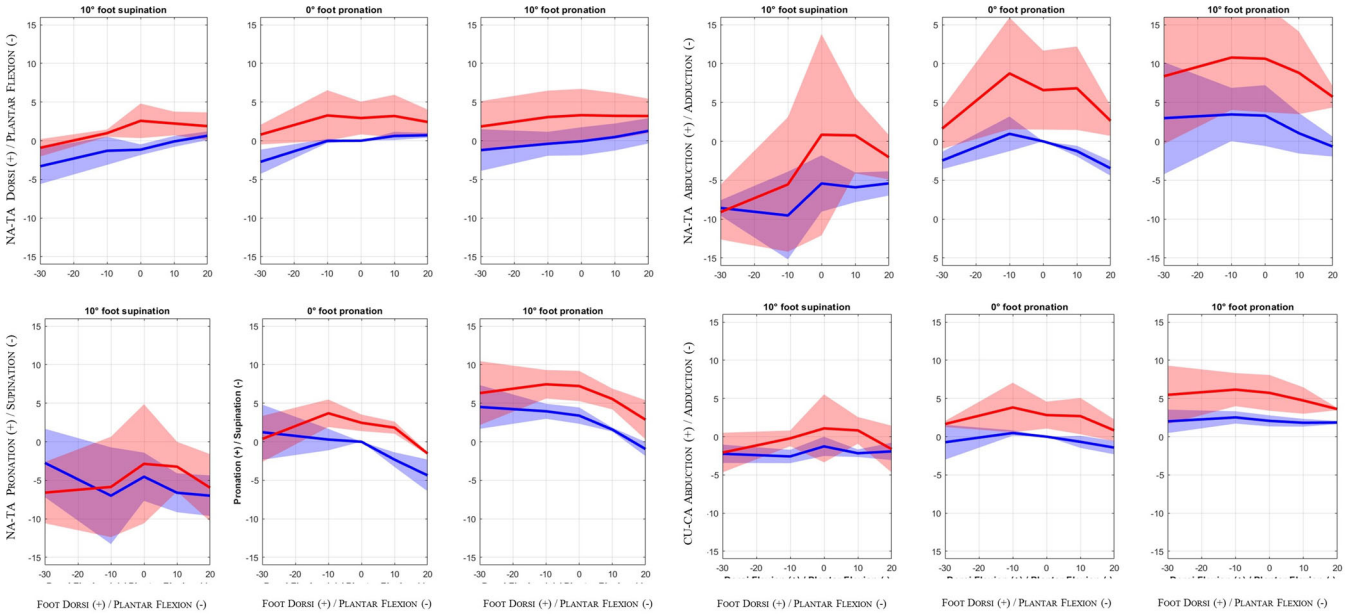

FIGURE 8 Statistically significant differences between nonweightbearing and weightbearing average rotational mobility for the main motion components at the Chopart joint.

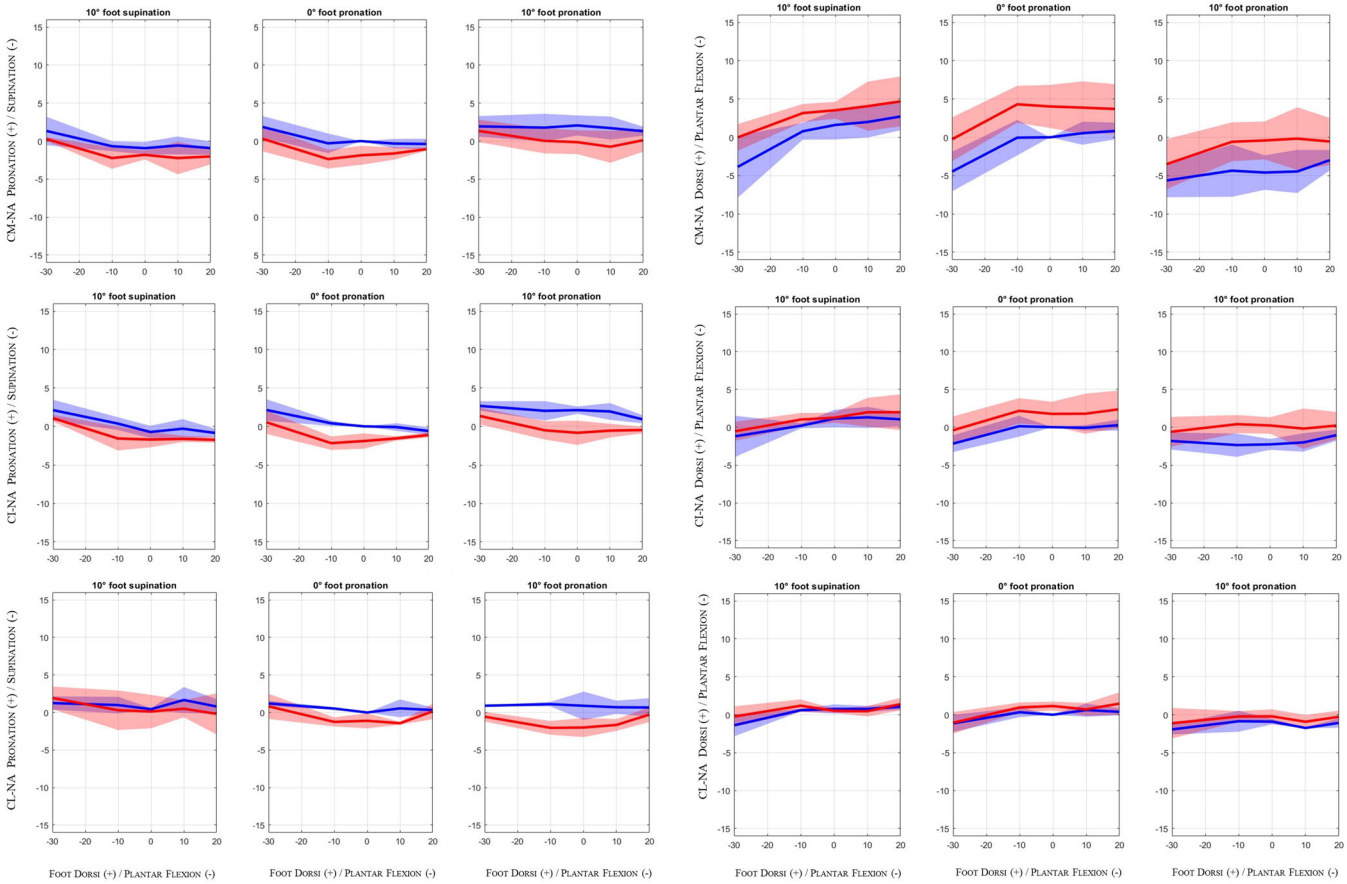

FIGURE 9 Statistically significant differences between nonweightbearing and weightbearing average rotational mobility for the main motion components at the cuneiforms.

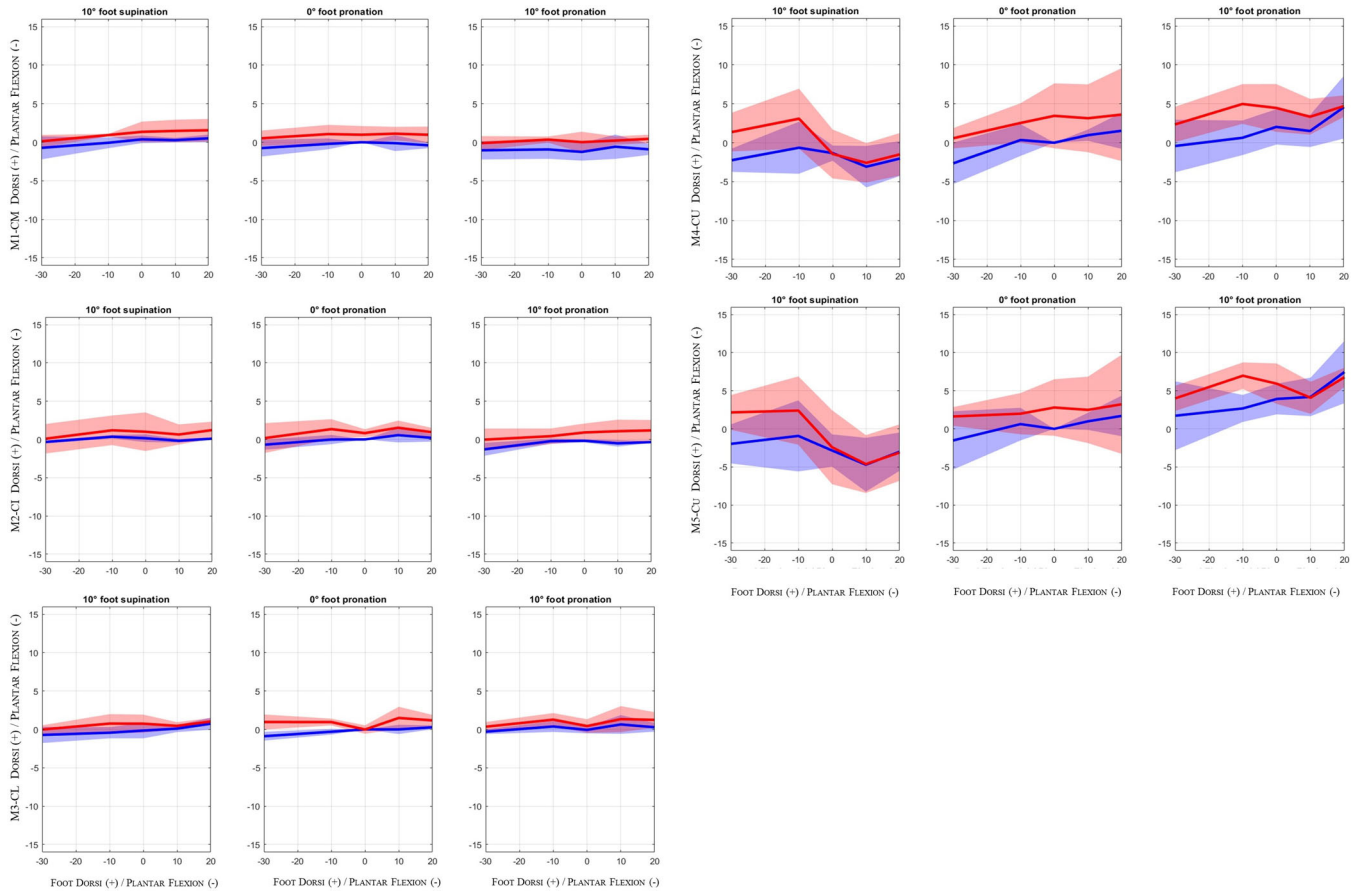

FIGURE 10 Statistically significant differences between nonweightbearing and weightbearing average flexion mobility at the metatarsal bones.

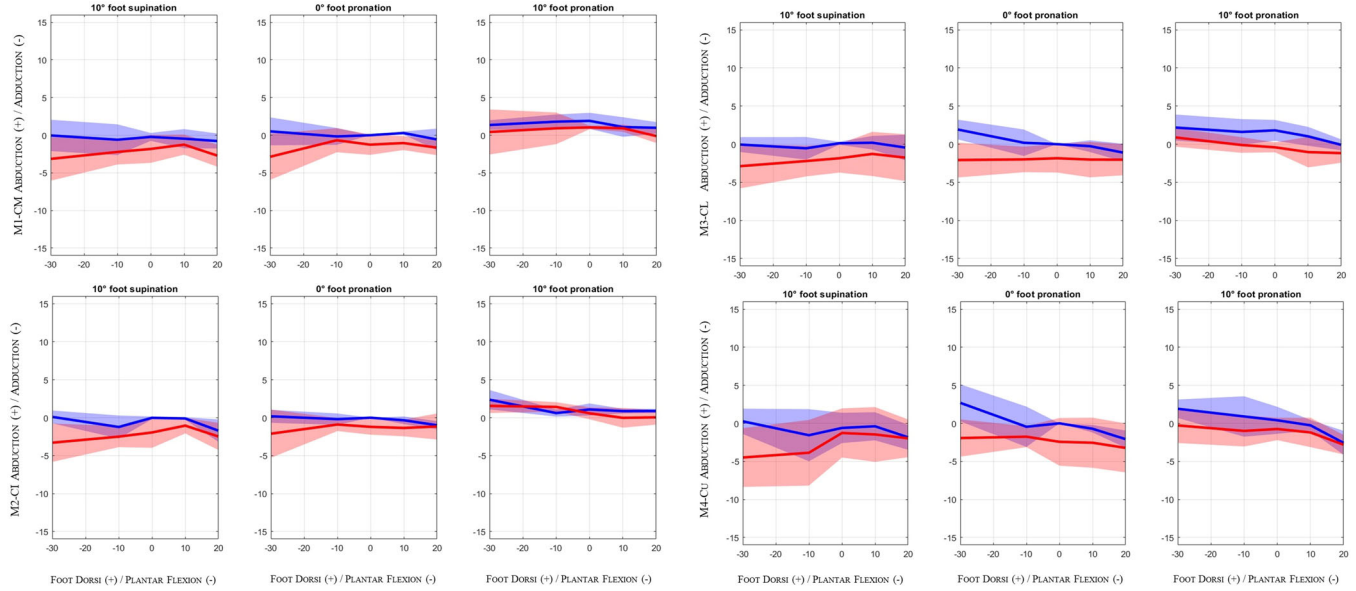

FIGURE 11 Statistically significant differences between nonweightbearing and weightbearing average abduction mobility at the metatarsal bones.

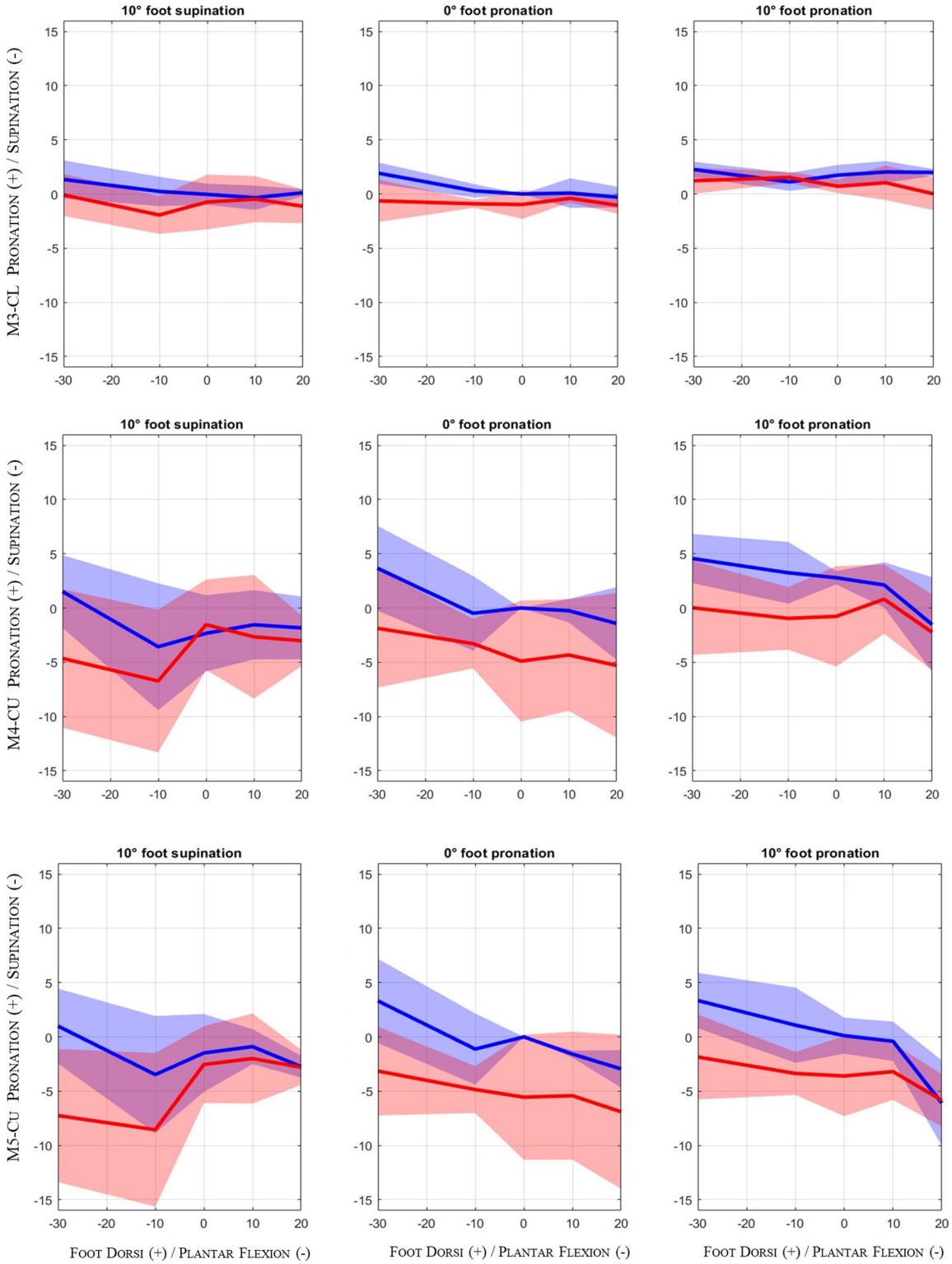

FIGURE 12 Statistically significant differences between nonweightbearing and weightbearing average pronation mobility at the metatarsal bones.

comparison. Some differences are, however, observable. With respect to in vivo data during gait,[27] we measured less fibular motion, possibly due to the lack of muscle activation during walk (Table S2). On the contrary, TA-TI, CA-TA, and NA-TA ROM are greater in our analysis (Table S2), reasonably as a consequence of having a wider range of foot pronation/supination with respect to.[27] The remaining ROM are substantially similar in the two studies. Despite performed in vitro, our analysis is thus compatible with what observed in vivo during slow-dynamic functional tasks. When compared with in vitro simulated gait data,[26] again we observed

more mobility at talus, calcaneus and navicular bone. However, in[26] talus abduction was almost three times and calcaneus flexion twice bigger than what reported in this study (Table S2). Moreover, in the study of Nester and co-workers, the ROM of some motion components of the cuneiforms and metatarsal bones were slightly higher than in our study (Table S3). These differences may possibly arise from the artificial muscle activation pattern used to guide the walking simulator, possibly altering the foot posture during gait with respect to in vivo case and to our investigation. This confirms how the foot motion under load deserve further attention, as both external and internal loads may significantly alter the foot kinematics.

The proposed ARS and TPRS, shown in Figure 3, represented foot bone kinematics with considerable different motion components. The present comparison enlightens the impact of reference system choice on the characterization of foot bone motion. With respect to TPRS, the proposed ARS minimize the cross-talk among motion components, thanks to a more physiological alignment among motion axes and bone reference systems. The effect is particularly evident for the subtalar joint: with ARS, the alignment between the antero-posterior axis of the calcaneus and the mean helical axis of the subtalar motion minimized the projection of rotations on secondary axes, resulting in an almost pure pronation/supination motion of CA-TA (Figure 4). On the contrary, TPRS resulted in considerable cross-talk among rotational the components (Figure S3), AS also observable in.[37] Similar observation holds for the NA-TA motion: ARS localize most of the rotational mobility on abduction/adduction, while TPRS distribute NA-TA mobility on the three axes of rotation. This effect is less evident for midtarsal and tarsal bones, due to both the similarity between ARS and TPRS orientation (Figure 3) and the smaller ROM. Moreover, ARS also allow the absolute description of the foot posture, while the TPRS approach only investigates the variation with respect to the neutral foot, where all rotational coordinates are set to zero. This considerably limits the comparison among different populations: for example, a healthy and a flat neutral foot are indistinguishable with TPRS, having the same initial orientation for all reference systems. As a more qualitative observation, being directly connected with bone anatomy, ARS provide an easier definition and interpretation of foot bone kinematics and clinical indicators, such as the medial longitudinal arch quantification presented in Conconi et al.[33]

This study has limitations. We analysed only three specimens. This was dictated by the number of bones and poses investigated in this study, resulting in a total of 448 bone models to be segmented. The statistical significance of our finding would benefit of a wider population; however, our findings are in line with previous study, supporting their general validity. In vitro tests may not fully represent the in vivo behavior of the foot and ankle complex. Yet, the quantification of the ROM in the absence of muscular activation is clinically relevant, as it represents the baseline condition from which deformation take place once muscle loads are applied. In this sense, differences between our in vitro quantification and what observed on low-dynamics task should be minor, as indeed observed when comparing our results with what reported in.[27] We had to resect the Achilles' tendon to restore physiological range of dorsi/plantar flexion. This clearly altered the integrity of the system, but was the only variation with respect to the otherwise intact leg. The Achilles tendon is, however, mainly responsible for the transmission of muscle forces, a parameter not included in this study. In this perspective, its resection could be considered as acceptable. Moreover, in many in vitro study soft tissues are cut below the knee level, resulting in boundary condition similar to those of here presented. The considered weightbearing scenario represent a very limited subset with respect to what experience by the foot during functional tasks, in terms of external load and even more in terms of internal loads due to muscles. It is thus reasonable to expect wider ROM during active, dynamic task such as running or jumping. As said, this point will deserve specific investigations.

Future work will aim at extending our analysis to other specimens and to repeat the analysis in vivo by means of a new dynamic MRI approach currently under development at our research group.[40]

AUTHOR CONTRIBUTIONS

Michele Conconi, Nicola Sancisi, Claudio Belvedere, and Alberto Leardini: designed the study. **Michele Conconi, Alessandro Pompili, Nicola Sancisi, Claudio Belvedere, and Stefano Durante**: collected the data. **Michele Conconi and Alessandro Pompili**: processed, analysed, and interpreted the data. **Michele Conconi and Alessandro Pompili**: drafted the paper. All authors have read, contribute, and approved the final submitted manuscript.

ACKNOWLEDGMENTS

This study was partially funded by the Italian Ministry of Health under the "5 per mille" program. None of the authors received any funding or financial support that could be perceived as bias in this research.

ORCID

Michele Conconi http://orcid.org/0000-0003-2392-2684
Claudio Belvedere http://orcid.org/0000-0003-4258-2267

REFERENCES

1. Fick R. *Handbuch der Anatomie und Mechanik der Gelenke. 111: Spezielle Gelenk- und Muskelmechanik*. Gustav Fischer, 593-653.
2. Manter JT. Movements of the subtalar and transverse tarsal joints. *Anat Rec*. 1941;80(4):397-410.
3. Hicks JH. The mechanics of the foot. *J Anat*. 1953;87(Pt.4):345-357.
4. Isman RE, Inman VT. Anthropometric studies of the human foot. *Bull Prosthet Res*. 1969;11(10):97-129. https://books.google.it/books?hl=it&lr=&id=KECHhkY2LSAC&oi=fnd&pg=PA97&dq=anthropometric+studies+of+the+human+foot&ots=mVJy5kUnF0&sig=-NxXpORwSejqoChJIrK0fRYvAbk&redir_esc=y#v=onepage&q=anthropometric%20studies%20of%20the%20human%20foot&f=false
5. Sammarco GJ, Burstein AH, Frankel VH. Biomechanics of the ankle: a kinematic study. *Orthop Clin North Am*. 1973;4(1):75-96.
6. Engsberg JR. A biomechanical analysis of the talocalcaneal joint—in vitro. *J Biomech*. 1987;20(4):429-442.

7. Siegler S, Chen J, Schneck CD. The three-dimensional kinematics and flexibility characteristics of the human ankle and subtalar joints—Part I: kinematics. *J Biomech Eng*. 1988;110(4):364-373.
8. Lundberg A. Kinematics of the ankle and foot: in vivo roentgen stereophotogrammetry. *Acta Orthop Scand*. 1989;60(sup233):1-26.
9. Lundberg A, Svensson OK. The axes of rotation of the talocalcaneal and talonavicular joints. *The Foot*. 1993;3(2):65-70.
10. Leardini A, Caravaggi P, Theologis T, Stebbins J. Multi-segment foot models and their use in clinical populations. *Gait Posture*. 2019;69:50-59.
11. Carson MC, Harrington ME, Thompson N, O'Connor JJ, Theologis TN. Kinematic analysis of a multi-segment foot model for research and clinical applications: a repeatability analysis. *J Biomech*. 2001;34(10):1299-1307.
12. Leardini A, Benedetti MG, Berti L, Bettinelli D, Nativo R, Giannini S. Rear-foot, mid-foot and fore-foot motion during the stance phase of gait. *Gait Posture*. 2007;25(3):453-462.
13. Ye D, Sun X, Zhang C, et al. In vivo foot and ankle kinematics during activities measured by using a dual fluoroscopic imaging system: a narrative review. *Front Bioeng Biotechnol*. 2021;9:693806. doi:10.3389/fbioe.2021.693806
14. Ito K, Hosoda K, Shimizu M, et al. Direct assessment of 3D foot bone kinematics using biplanar X-ray fluoroscopy and an automatic model registration method. *J Foot Ankle Res*. 2015;8(1):21.
15. Phan CB, Shin G, Lee KM, Koo S. Skeletal kinematics of the midtarsal joint during walking: midtarsal joint locking revisited. *J Biomech*. 2019;95:109287.
16. Balsdon MER, Bushey KM, Dombroski CE, LeBel ME, Jenkyn TR. Medial longitudinal arch angle presents significant differences between foot types: a biplane fluoroscopy study. *J Biomech Eng*. 2016;138(10):101007. doi:10.1115/1.4034463
17. Kessler SE, Rainbow MJ, Lichtwark GA, et al. A direct comparison of biplanar videoradiography and optical motion capture for foot and ankle kinematics. *Front Bioeng Biotechnol*. 2019;7:199.
18. Siegler S, Udupa JK, Ringleb SI, et al. Mechanics of the ankle and subtalar joints revealed through a 3D quasi-static stress MRI technique. *J Biomech*. 2005;38(3):567-578.
19. Goto A, Moritomo H, Itohara T, Watanabe T, Sugamoto K. Three-dimensional in vivo kinematics of the subtalar joint during dorsiplantarflexion and inversion–eversion. *Foot Ankle Int*. 2009;30(5):432-438.
20. Fassbind MJ, Rohr ES, Hu Y, et al. Evaluating foot kinematics using magnetic resonance imaging: from maximum plantar flexion, inversion, and internal rotation to maximum dorsiflexion, eversion, and external rotation. *J Biomech Eng*. 2011;133(10):104502. doi:10.1115/1.4005177
21. Sheehan FT, Seisler AR, Siegel KL. In vivo talocrural and subtalar kinematics: a non-invasive 3D dynamic MRI study. *Foot Ankle Int*. 2007;28(3):323-335.
22. Makki K, Borotikar B, Garetier M, Brochard S, Ben Salem D, Rousseau F. In vivo ankle joint kinematics from dynamic magnetic resonance imaging using a registration-based framework. *J Biomech*. 2019;86:193-203.
23. Borotikar B, Lempereur M, Lelievre M, Burdin V, Ben Salem D, Brochard S. Dynamic MRI to quantify musculoskeletal motion: A systematic review of concurrent validity and reliability, and perspectives for evaluation of musculoskeletal disorders. *PLoS One*. 2017;12(12):e0189587.
24. Arndt A, Westblad P, Winson I, Hashimoto T, Lundberg A. Ankle and subtalar kinematics measured with intracortical pins during the stance phase of walking. *Foot Ankle Int*. 2004;25(5):357-364.
25. Nester C, Jones RK, Liu A, et al. Foot kinematics during walking measured using bone and surface mounted markers. *J Biomech*. 2007;40(15):3412-3423.
26. Nester CJ, Liu AM, Ward E, et al. In vitro study of foot kinematics using a dynamic walking cadaver model. *J Biomech*. 2007;40(9):1927-1937.
27. Lundgren P, Nester C, Liu A, et al. Invasive in vivo measurement of rear-, mid-and forefoot motion during walking. *Gait Posture*. 2008;28(1):93-100.
28. Whittaker EC, Aubin PM, Ledoux WR. Foot bone kinematics as measured in a cadaveric robotic gait simulator. *Gait Posture*. 2011;33(4):645-650.
29. Kaneda K, Harato K, Oki S, et al. Three-dimensional kinematic change of hindfoot during full weightbearing in standing: an analysis using upright computed tomography and 3D-3D surface registration. *J Orthop Surg*. 2019;14(1):355.
30. Ito K, Hosoda K, Shimizu M, et al. Three-dimensional innate mobility of the human foot bones under axial loading using biplane X-ray fluoroscopy. *R Soc Open Sci*. 2017;4(10):171086.
31. Lenz AL, Strobel MA, Anderson AM, et al. Assignment of local coordinate systems and methods to calculate tibiotalar and subtalar kinematics: a systematic review. *J Biomech*. 2021;120:110344.
32. Brown JA, Gale T, Anderst W. An automated method for defining anatomic coordinate systems in the hindfoot. *J Biomech*. 2020;109:109951.
33. Conconi M, Pompili A, Sancisi N, Leardini A, Durante S, Belvedere C. New anatomical reference systems for the bones of the foot and ankle complex: definitions and exploitation on clinical conditions. *J Foot Ankle Res*. 2021;14(1):66.
34. Tuijthof GJM, Zengerink M, Beimers L, et al. Determination of consistent patterns of range of motion in the ankle joint with a computed tomography stress-test. *Clinical Biomechanics*. 2009;24(6):517-523.
35. Grood ES, Suntay WJ. A joint coordinate system for the clinical description of three-dimensional motions: application to the knee. *J Biomech Eng*. 1983;105(2):136-144.
36. Fu Y, Liu S, Li H, Yang D. Automatic and hierarchical segmentation of the human skeleton in CT images. *Phys Med Biol*. 2017;62(7):2812-2833.
37. Yamaguchi S, Sasho T, Kato H, Kuroyanagi Y, Banks SA. Ankle and subtalar kinematics during dorsiflexion-plantarflexion activities. *Foot Ankle Int*. 2009;30(4):361-366.
38. Huber T, Schmoelz W, Bölderl A. Motion of the fibula relative to the tibia and its alterations with syndesmosis screws: a cadaver study. *Foot Ankle Surg*. 2012;18(3):203-209.
39. Leardini A, Durante S, Belvedere C, et al. Weight-bearing CT technology in musculoskeletal pathologies of the lower limbs: techniques, initial applications, and preliminary combinations with gait-analysis measurements at the istituto ortopedico rizzoli. *Semin Musculoskelet Radiol*. 2019;23(6):643-656.
40. Conconi M, De Carli F, Berni M, Sancisi N, Parenti-Castelli V, Monetti G. In-vivo quantification of knee deep-flexion in physiological loading condition trough dynamic MRI. *Applied Sciences*. 2023;13:629.

SUPPORTING INFORMATION

Additional supporting information can be found online in the Supporting Information section at the end of this article.

How to cite this article: Conconi M, Pompili A, Sancisi N, Durante S, Leardini A, Belvedere C. Foot kinematics as a function of ground orientation and weightbearing. *J Orthop Res*. 2024;42:148-163. doi:10.1002/jor.25661